A Selection from

Smithsonian at the Poles

Contributions to International Polar Year Science

Igor Krupnik, Michael A. Lang, and Scott E. Miller
Editors

A Smithsonian Contribution to Knowledge

Smithsonian Institution
Scholarly Press
WASHINGTON, D.C.
2009

This proceedings volume of the Smithsonian at the Poles symposium, sponsored by and convened at the Smithsonian Institution on 3–4 May 2007, is published as part of the International Polar Year 2007–2008, which is sponsored by the International Council for Science (ICSU) and the World Meteorological Organization (WMO).

Published by Smithsonian Institution Scholarly Press

P.O. Box 37012
MRC 957
Washington, D.C. 20013-7012
www.scholarlypress.si.edu

Cover design: Piper F. Wallis

Cover images: (top left) Wave-sculpted iceberg in Svalbard, Norway (Photo by Laurie M. Penland); (top right) Smithsonian Scientific Diving Officer Michael A. Lang prepares to exit from ice dive (Photo by Adam G. Marsh); (main) Kongsfjorden, Svalbard, Norway (Photo by Laurie M. Penland).

Library of Congress Cataloging-in-Publication Data

Smithsonian at the poles : contributions to International Polar Year science / Igor Krupnik, Michael A. Lang, and Scott E. Miller, editors.
p. cm.
ISBN 978-0-9788460-1-5 (pbk. : alk. paper)
1. International Polar Year, 2007–2008. 2. Polar regions—Research—Congresses. 3. Research—Polar regions—Congresses. 4. Arctic regions—Research—Congresses. 5. Antarctica—Research—Congresses. 6. Polar regions—Environmental conditions—Congresses. 7. Climatic changes—Detection—Polar regions—Congresses. I. Krupnik, Igor. II. Lang, Michael A. III. Miller, Scott E.

G587.S65 2009
559.8—dc22 2008042055

ISBN-13: 978-0-9788460-1-5
ISBN-10: 0-9788460-1-X

Chromophoric Dissolved Organic Matter Cycling during a Ross Sea *Phaeocystis antarctica* Bloom

David J. Kieber, Dierdre A. Toole, and Ronald P. Kiene

ABSTRACT. Chromophoric dissolved organic matter (CDOM) is ubiquitous in the oceans, where it is an important elemental reservoir, a key photoreactant, and a sunscreen for ultraviolet (UV) radiation. Chromophoric dissolved organic matter is generally the main attenuator of UV radiation in the water column, and it affects the remote sensing of chlorophyll *a* (chl *a*) such that corrections for CDOM need to be incorporated into remote sensing algorithms. Despite its significance, relatively few CDOM measurements have been made in the open ocean, especially in polar regions. In this paper, we show that CDOM spectral absorption coefficients (a_λ) are relatively low in highly productive Antarctic waters, ranging from approximately 0.18 to 0.30 m^{-1} at 300 nm and 0.014 to 0.054 m^{-1} at 443 nm. These values are low compared to coastal waters, but they are higher (by approximately a factor of two to three) than a_λ in oligotrophic waters at low latitudes, supporting the supposition of a poleward increase in a_{CDOM} in the open ocean. Chromophoric dissolved organic matter a_λ and spectral slopes did not increase during the early development of a bloom of the colonial haptophyte *Phaeocystis antarctica* in the Ross Sea, Antarctica, even though chl *a* concentrations increased more than one-hundred-fold. Our results suggest that Antarctic CDOM in the Ross Sea is not coupled directly to algal production of organic matter in the photic zone during the early bloom but is rather produced in the photic zone at a later time or elsewhere in the water column, possibly from organic-rich sea ice or the microbial degradation of algal-derived dissolved organic matter exported out of the photic zone. Spectral a_λ at 325 nm for surface waters in the Southern Ocean and Ross Sea were remarkably similar to values reported for deep water from the North Atlantic by Nelson et al. in 2007. This similarity may not be a coincidence and may indicate long-range transport to the North Atlantic of CDOM produced in the Antarctic via Antarctic Intermediate and Bottom Water.

David J. Kieber, Department of Chemistry, State University of New York College of Environmental Science and Forestry, Syracuse, NY 13210, USA. Dierdre A. Toole, Department of Marine Chemistry and Geochemistry, Woods Hole Oceanographic Institution, Woods Hole, MA 02543, USA. Ronald P. Kiene, Department of Marine Sciences, University of South Alabama, Mobile, AL 36688, USA. Corresponding author: D. Kieber (djkieber@esf.edu). *Accepted 28 May 2008.*

INTRODUCTION

Quantifying temporal and spatial variations in chromophoric dissolved organic matter (CDOM) absorption is important to understanding the biogeochemistry of natural waters because CDOM plays a significant role in determining the underwater light field. Chromophoric dissolved organic matter is the fraction of dissolved organic matter (DOM) that absorbs solar radiation in natural waters, including radiation in the UVB (280 to 320 nm), the UVA (320 to 400 nm), and the visible portion (400 to 700 nm) of the solar spectrum. For most natural waters, CDOM is the primary constituent that attenuates actinic

UVB and UVA radiation in the water column. Consequently, CDOM acts as a "sunscreen," providing protection from short wavelengths of solar radiation that can be damaging to aquatic organisms (Hebling and Zagarese, 2003). Chromophoric dissolved organic matter absorption is often also quite high in the blue spectral region, particularly in the subtropics and poles, accounting for a quantitatively significant percentage of total nonwater absorption (Siegel et al., 2002), complicating remote sensing of phytoplankton pigment concentrations and primary productivity (Carder et al., 1989; Nelson et al., 1998). In lakes and coastal areas with high riverine discharge, CDOM absorption in the blue region can be so large as to restrict phytoplankton absorption of light, thereby placing limits on primary productivity (e.g., Vodacek et al., 1997; Del Vecchio and Blough, 2004). Since CDOM absorption affects the satellite-retrieved phytoplankton absorption signal in most oceanic waters, especially coastal waters, CDOM absorption must be accounted for when using remotely sensed data (Blough and Del Vecchio, 2002). This necessitates a thorough understanding of the characteristics of CDOM and factors controlling its distribution in different areas of the ocean.

Sources of CDOM in the oceans are varied and, in many cases, poorly described. Potential sources include terrestrial input of decaying plant organic matter, autochthonous production by algae, photochemical or bacterial processing of DOM, and release from sediments (e.g., Blough et al., 1993; Opsahl and Benner, 1997; Nelson et al., 1998; Nelson and Siegel, 2002; Rochelle-Newall and Fisher, 2002a, 2002b; Chen et al., 2004; Nelson et al., 2004). The removal of CDOM in the oceans is dominated by its photochemical bleaching, but microbial processing is also important although poorly understood (Blough et al., 1993; Vodacek et al., 1997; Del Vecchio and Blough, 2002; Chen et al., 2004; Nelson et al., 2004; Vähätalo and Wetzel, 2004).

Absorption of sunlight by CDOM can affect an aquatic ecosystem both directly and indirectly (Schindler and Curtis, 1997). The bleaching of CDOM absorption and fluorescence properties as a result of sunlight absorption lessens the biological shielding effect of CDOM in surface waters. Chromophoric dissolved organic matter photobleaching may also produce a variety of reactive oxygen species (ROS), such as the hydroxyl radical, hydrogen peroxide, and superoxide (for review, see Kieber et al., 2003). Generation of these compounds provides a positive feedback to CDOM removal by causing further destruction of CDOM via reaction with these ROS.

Although CDOM has been intensively studied to understand its chemical and physical properties, previous research has primarily focused on CDOM cycling in temperate and subtropical waters. Very little is known regarding temporal and spatial distributions of CDOM in high-latitude marine waters. Studies in the Bering Strait–Chukchi Sea region and the Greenland Sea showed that absorption coefficients (a_λ) and spectral slopes (S) derived from CDOM absorption spectra at coastal stations were influenced by terrestrial inputs and comparable to a_λ and S values in temperate and tropical coastal sites (Stedmon and Markager, 2001; Ferenac, 2006). As the distance from the coastline in the Bering Strait and Chukchi Sea proper increased, there was a large decrease in a_λ from 1.5 to 0.2 m^{-1} at 350 nm. These a_λ were mostly higher than a_{350} observed in the open ocean at lower latitudes (Ferenac, 2006). However, corresponding spectral slopes were significantly lower ($\leq$0.014 nm^{-1}) than open oceanic values in the Sargasso Sea and elsewhere ($\geq$0.02 nm^{-1}; Blough and Del Vecchio, 2002), suggesting that the types of CDOM present in these contrasting environments were different, possibly owing to a residual terrestrial signal and lower degree of photobleaching in the Arctic samples.

As with Arctic waters, there is very little known regarding CDOM in Antarctic waters. To our knowledge, there are only three published reports investigating CDOM distributions in the Ross Sea and along the Antarctic Peninsula (Sarpal et al., 1995; Patterson, 2000; Kieber et al., 2007). A key finding of the Sarpal et al. study was that Antarctic waters were quite transparent in the UV ($a_\lambda < 0.4$ m^{-1} at $\lambda \geq$ 290 nm), even at coastal stations during a bloom of *Cryptomonas* sp. Patterson (2000) examined CDOM in several transects perpendicular to the Antarctic Peninsula coastline and found that CDOM absorption coefficients were low in the austral summer, with a_{305} ($\pm$SD) = 0.28 ($\pm$0.09) m^{-1} and a_{340} = 0.13 ($\pm$0.06) m^{-1}. Similarly low a_λ were observed by Kieber et al. (2007) in the upper water column of the Ross Sea ($a_{300} \sim 0.32$ m^{-1} and $a_{350} \sim 0.15$ m^{-1}) during the end of a *Phaeocystis antarctica* bloom when diatoms were also blooming (chl $a \sim 3.8$ μg L^{-1}).

Polar regions are unique in many ways that may influence CDOM optical properties. Sea ice may provide a rich source of ice-derived CDOM to melt water (Scully and Miller, 2000; Xie and Gosselin, 2005). Additionally, polar blooms can decay without significant losses to zooplankton, especially in the spring when zooplankton grazing can be minimal (Caron et al., 2000; Overland and Stabeno, 2004; Rose and Caron, 2007).

In the Ross Sea, soon after the opening of the Ross Sea polynya in the austral spring, a *Phaeocystis antarctica*–dominated bloom regularly occurs (Smith et al., 2000), especially in waters away from the ice edge where iron

concentrations are lower and the water column is more deeply mixed. As is typical of polar regions, the massive phytoplankton production that is observed during the early stages of this bloom (in the early to mid austral spring) is not accompanied by significant micro- or macrozooplankton grazing (Caron et al., 2000). The spring bloom also appears to be a period of low bacterial abundance and activity (Ducklow et al., 2001), although bacteria do bloom during the later stages of the algal bloom, in early to mid summer, coinciding with an increase in dissolved and particulate organic carbon (Carlson et al., 2000).

Depending on physiological and hydrodynamic factors, this ecological decoupling between primary productivity and both microbial productivity and grazing may cause the phytoplankton to sink out of the photic zone (DiTullio et al., 2000; Becquevort and Smith, 2001; Overland and Stabeno, 2004). This may lead to a significant flux of organic matter to the ocean floor and to deepwater CDOM production. Export of the phytoplankton out of the photic zone may also lead to a decoupling of bloom dynamics and CDOM cycling.

Here we report on spatial and temporal patterns in CDOM spectra observed during the early stages of the 2005 austral spring *Phaeocystis antarctica* bloom in the seasonal Ross Sea polynya. Our results show that CDOM changed very little during a period when chl *a* concentrations increased more than one-hundred-fold. Implications of this finding for CDOM cycling in the Ross Sea are discussed.

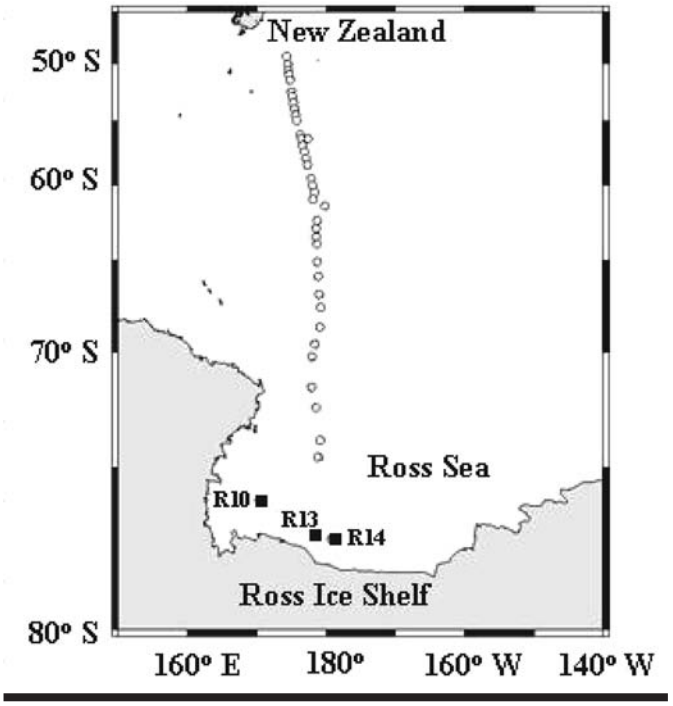

FIGURE 1. Locations of transect sampling stations south of New Zealand to the Ross Sea (open circles) and the main hydrographic stations that were occupied in the Ross Sea (solid black circles) during the NBP05-08 cruise. Latitude and longitude information for specific hydrographic stations (e.g., R10A and R10D) are given in figure captions 4, 5, 8 and 9.

METHODS

Ross Sea Site Description and Sampling

A field campaign was conducted aboard the R/V *Nathaniel B. Palmer* in the seasonal ice-free polynya in the Ross Sea, Antarctica, from 8 November to 30 November 2005 (Figure 1). During this time, the surface seawater temperature was approximately –1.8°C and the phytoplankton assemblage was dominated by colonial *Phaeocystis antarctica*. Three main hydrographic stations were occupied within the Ross Sea polynya for approximately seven days each (i.e., R10, R13, R14). Seawater samples were collected from early morning hydrocasts (0400-0700 local time) directly from Niskin bottles attached to a conductivity, temperature, and depth (CTD) rosette. Vertical profiles of a suite of routine measurements were obtained at each station including downwelling irradiance (and coupled incident surface irradiance), chl *a*, and CDOM absorption spectra. Additionally, a profile of dissolved organic carbon (DOC) was collected at one station (14F).

In addition to studying CDOM cycling in the Ross Sea, we also collected and analyzed surface water CDOM samples during our North-South transit from New Zealand through the Southern Ocean to the Ross Sea (28 October–7 November, 2005). Transect sampling for CDOM was conducted from ~49 to ~75°S. Details of the cruise track, sampling protocols, analyses conducted and meteorological and sea ice conditions for the southbound transect are presented in Kiene et al. (2007). The transect encompassed open waters of the Southern Ocean, the northern sea-ice melt zone, and ice-covered areas near the northern Ross Sea.

Chlorophyll *a* was determined fluorometrically by employing the acidification method described by Strickland and Parsons (1968). Briefly, 50–250 mL of seawater was filtered onto a 25-mm GF/C glass fiber filter (Whatman Inc., Floram Park, New Jersey) with low vacuum. Filters were placed in 5 mL of 90% HPLC-grade acetone and extracted for 24 h at –20°C. Chlorophyll fluorescence in the acetone extracts was quantified with a Turner Designs 10-AU fluorometer (Sunnyvale, Calafornia) before and after 80-μL addition of 10% HCl. Dissolved organic carbon samples were

collected and concentrations were determined by employing the techniques outlined in Qian and Mopper (1996).

For nutrient and CDOM samples, seawater was collected directly from Niskin bottles by gravity filtration through a 20-μm Nitex mesh (held in a 47-mm-diameter polycarbonate (PC) filter holder) followed by a precleaned 0.2-μm AS 75 Polycap filter capsule (nylon membrane with a glass microfiber prefilter enclosed in a polypropylene housing). Silicone tubing was used to attach the PC filter to the Niskin bottle spigot and the Polycap to the PC filter outlet. Nutrient samples were collected into 50-mL polypropylene centrifuge tubes, while samples for CDOM were filtered into precleaned 80-mL Qorpak bottles sealed with Teflon-lined caps (see Toole et al., 2003, for details regarding sample filtration and glassware preparation). Nutrient samples were stored frozen at −80°C until shipboard analysis by standard flow-injection techniques.

CDOM Absorption Spectra

Absorbance spectra were determined with 0.2-μm filtered seawater samples that were warmed to room temperature in the dark immediately after they were collected and then analyzed soon thereafter (generally within 24 h). Absorbance spectra were determined in a 100-cm path length, Type II liquid capillary waveguide (World Precision Instruments) attached to an Ocean Optics model SD2000 dual-channel fiber-optic spectrophotometer and a Micropack DH 2000 UV-visible light source. Prior to analysis, a sample or blank was first deaerated with ultrahigh purity He in an 80-mL Qorpak bottle and then pulled through the capillary cell slowly with a Rainin Rabbit peristaltic pump. Deaeration with He eliminated bubble formation in the sample cell, while increasing the pH slightly from 8.0 to 8.3. This pH change is not expected to affect absorption spectra, although this was not explicitly tested. The reference solution consisted of 0.2-μm-filtered 0.7-*M* NaCl prepared from precombusted (600°C, 24 h) high-purity sodium chloride (99.8%, Baker Analyzed) and dissolved in high-purity (18.2 MΩ cm) laboratory water obtained from a Millipore Milli-Q ultrapure water system (Millipore Corp., Billerica, Massachusetts). The sodium chloride solution was used to approximately match the ionic strength of the Ross Sea seawater samples and minimize spectral offsets due to refractive index effects. Even though a sodium chloride solution was used as a reference, sample absorbance spectra still exhibited small, variable baseline offsets (~0.005 AU). This was corrected for by adjusting the absorbance (A_λ) to zero between 650 and 675 nm where the sample absorbance was assumed to be zero. The capillary cell was flushed after every fourth or fifth seawater sample with deaerated Milli-Q water and high-purity, distilled-in-glass-grade methanol (Burdick and Jackson, Muskegon, Michigan). Corrected absorbance values were used to calculate absorption coefficients:

$$a_\lambda = 2.303 A_\lambda / l, \tag{1}$$

where l is the path length of the capillary cell. Each sample was analyzed in triplicate, resulting in ≤2% relative standard deviation (RSD) in spectral absorbance values ≤400 nm. On the basis of three times the standard deviation of the sodium chloride reference, the limit of detection for measured absorption coefficients was approximately 0.002 m^{-1}. To characterize sample absorption, spectra were fit to the following exponential form (e.g., Twardowski et al., 2004):

$$a_\lambda = a_{\lambda o}\, e^{-S(\lambda - \lambda o)}, \tag{2}$$

where $a_{\lambda o}$ is the absorption coefficient at the reference wavelength, λ_o, and S is the spectral slope (nm^{-1}). Data were fit to a single exponential equation using SigmaPlot (SPSS Inc.). Slope coefficients were evaluated from 275 to 295 nm ($S_{275–295}$; λ_o = 285 nm) and from 350 to 400 nm ($S_{350–400}$; λ_o = 375 nm). These wavelength ranges were selected for study of spectral slopes instead of using broader wavelength ranges (e.g., 290–700 nm) because the former can be measured with high precision and better reflects biogeochemical changes in CDOM in the water column (Helms et al., 2008).

Optical Profiles

Vertical profiles of spectral downwelling irradiance ($E_d(z,\lambda)$) and upwelling radiance ($L_u(z,\lambda)$), as well as the time course of surface irradiance ($E_d(0^+,\lambda, t)$), were determined separately for ultraviolet and visible wavebands. Ultraviolet wavelengths were sampled using a Biospherical Instruments, Inc. (BSI, San Diego, California) PUV-2500 Profiling Ultraviolet Radiometer coupled with a continuously sampling, deck-mounted, cosine-corrected GUV-2511 Ground-based Ultraviolet Radiometer. Both sensors had a sampling rate of approximately 6 Hz and monitored seven channels centered at 305, 313, 320, 340, 380, and 395 nm, as well as integrated photosynthetically active radiation (PAR). Each channel had an approximate bandwidth of 10 nm, except for the 305-nm channel, whose bandwidth was determined by the atmospheric ozone cutoff and the PAR channel, which monitored the irradiance

from 400 to 700 nm. The irradiance at several visible wavelength channels, centered at 412, 443, 490, 510, 555, and 665 nm, as well as PAR, were determined with a BSI PRR-600 Profiling Reflectance Radiometer coupled to a radiometrically matched surface reference sensor (PRR-610). Similarly, both PRR sensors had a sampling rate of approximately 6 Hz and an approximate bandwidth of 10 nm. The PUV-2500 was deployed multiple times a day (generally, three to five profiles per day) in free-fall mode, allowing it to sample at a distance of over 10 m from the ship, minimizing effects from ship shadow and instrument tilt (Waters et al., 1990). The PRR-600 was deployed several times per station in a metal lowering frame via the starboard side winch. Prior to each cast, the ship was oriented relative to the sun to minimize ship shadow. The GUV-2511 and PRR-610 were mounted to the deck, and care was taken to avoid shadows or reflected light associated with the ship's superstructure. To reduce instrument variability due to atmospheric temperature fluctuations, the GUV-2511 was equipped with active internal heating. All calibrations utilized coefficients provided by BSI, and the data were processed using standard procedures.

Spectral downwelling attenuation coefficients ($K_d(\lambda)$, m^{-1}) were derived from each PUV-2500 and PRR-600 profile as the slope of log-transformed $E_d(z, \lambda)$ versus depth. On the basis of water clarity, the depth interval for this calculation varied from < 10 m for shorter UV wavelengths up to 20-30 m for blue wavelengths of solar radiation. Daily mean $K_d(\lambda)$ were derived as the average of individual $K_d(\lambda)$ coefficients determined from each PUV and PRR profile, and station means were determined by averaging the daily $K_d(\lambda)$ coefficients.

RESULTS

Sample Storage and Spectral Comparison

A storage test was conducted with seawater collected on 29 October 2005 (52°59.90′S, 175°7.76′E) during the transect from New Zealand to the Ross Sea. The sample was obtained from the ship's underway pump system that had an intake depth at approximately 4 m. Seawater was filtered directly from the pump line through a 0.2-μm AS 75 Polycap filter capsule into an 80-mL Qorpak bottle and stored in the dark at room temperature. When this sample was analyzed multiple times over a period of two weeks ($n = 8$), no change was observed in its absorption spectrum with respect to spectral absorption coefficients or spectral slopes. For example, a_{300} varied over a very narrow range from 0.196 to 0.202 m^{-1} with a mean value of 0.197 m^{-1} and 3.1% RSD. This RSD is only slightly larger than the RSD for replicate analysis of the same sample when done sequentially (~2%). Likewise, the spectral slope from 275 to 295 nm ($S_{275\text{-}295}$) showed very little variation over time, ranging from 0.0337 to 0.0377 nm^{-1} (0.0358 nm^{-1} mean and 3.4% RSD). The $S_{350\text{-}400}$ varied somewhat more (11.8% RSD) due to the lower a_λ values, ranging from 0.0075 to 0.0111 nm^{-1}, with a mean value of 0.009 nm^{-1}. A storage study with two other samples that were collected along the transect showed similar results, with very little variability observed in either a_λ or S beyond the precision of sequential spectral measurements.

In addition to the storage study, absorption spectra obtained with the capillary waveguide system were compared to those obtained with the commonly used Perkin Elmer Lamda 18 dual-beam, grating monochromator spectrophotometer. There was no statistical difference in the spectral absorption coefficients obtained by these two spectrophotometers, except for considerably more noise in a_λ obtained with the Perkin Elmer spectrophotometer (Figure 2). The increased spectral noise seen with the Beckman spectrophotometer was expected due to the relatively short path length (0.10 m) and the extremely low absorbance values in the Ross Sea seawater samples (e.g., ~0.009 AU at 400 nm), which were close to the detection limit of this instrument. In contrast, a_λ spectra obtained

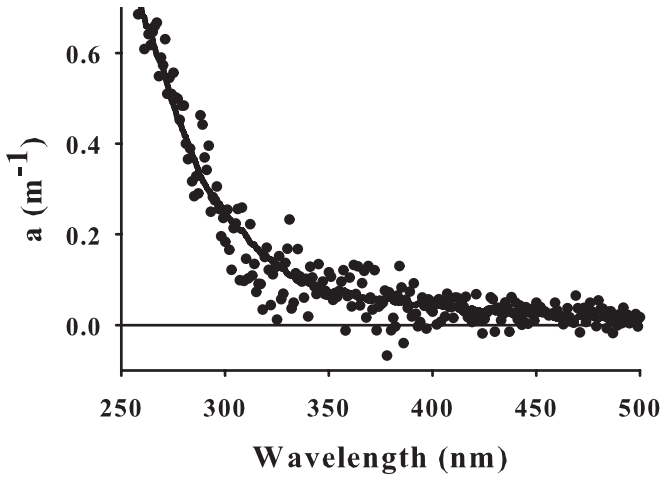

FIGURE 2. Comparison of spectral absorption coefficients determined with a Perkin-Elmer Lambda 18 dual-beam spectrophotometer (circles) and a capillary waveguide spectrophotometer (solid line). A 10-cm cylindrical quartz cell was used to obtain spectral absorption coefficients with the Perkin-Elmer spectrophotometer. Absorbance spectra were referenced against a 0.7 M NaCl solution.

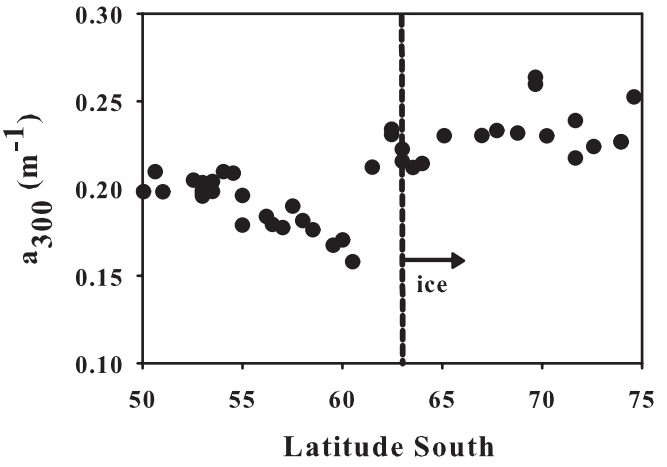

FIGURE 3. Sea surface a_{300} plotted as a function of degrees latitude south for the Oct–Nov 2005 transect from the Southern Ocean south of New Zealand to the Ross Sea. All data were obtained from water collected from the ship's underway seawater pump system (intake at approximately 4-m depth) that was filtered inline through a 0.2-μm AS 75 Polycap filter. The dashed line represents the approximate location of the northern extent of seasonal sea ice in our transect. For details regarding the transect, see Kiene et al. (2007).

with the capillary waveguide were much smoother owing to the much higher absorbance values due to the much longer path length (1 m) and the ability to spectrally average over several scans.

Transect and Ross Sea CDOM Absorption Spectra

Absorption coefficients obtained during our transect from New Zealand to the Ross Sea were generally low, as exemplified by a_{300} (Figure 3). Values for a_{300} ranged from 0.178 to 0.264 m^{-1}, with an average value of 0.209 m^{-1}. Interestingly, absorption coefficients at 300 nm were consistently higher in samples collected with significant ice cover (avg ± SD: 0.231 ± 0.014 m^{-1}) compared to a_{300} values collected in the Southern Ocean north of the sea ice (avg ± SD: 0.195 ± 0.017 m^{-1}) (Figure 3), possibly due to lower rates of photobleaching or release of CDOM from the sea ice into the underlying seawater (Scully and Miller, 2000; Xie and Gosselin, 2005). However, we cannot exclude the possibility that the ship caused some release of CDOM from the ice during our passage through it.

Absorption coefficients were also low within the Ross Sea during the development of the *Phaeocystis antarctica* bloom, even when surface waters were visibly green (chl a = 4–8 μg L^{-1}). For example, the absorption coefficient spectrum at station R14F was remarkably similar to that obtained in the Sargasso Sea during July 2004 (Figure 4), even though the chl *a* content of these two water samples differed by two orders of magnitude (7.0 versus 0.08 μg L^{-1}, respectively). The main differences observed between the two spectra were seen at wavelengths less than approximately 350 nm, with the Sargasso Sea sample exhibiting a much higher spectral slope (e.g., $S_{275–295}$ of 0.0466 versus 0.0273 nm^{-1}) and the Ross Sea sample having a higher a_λ between ~300 and 350 nm. These differences are likely due to different autochthonous sources of CDOM as well as the presence of micromolar levels of nitrate in the Antarctic sample (and perhaps dissolved mycosporine amino acids (MAA) as well; see "Ross Sea Temporal Trends in CDOM" section) compared to the low nanomolar levels of nitrate in the surface Sargasso Sea sample.

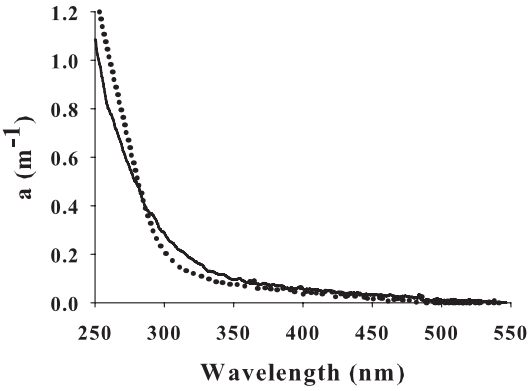

FIGURE 4. Comparison of spectral absorption coefficients determined with seawater collected from 50 m in the Sargasso Sea (30°55.5′N, 65°17.8′W) on 21 July 2004 (dotted line) and from 40 m in the Ross Sea (77°31.2′S, 179°79.8′W) on 26 November 2005 (station R14B, solid line). Both samples were 0.2-μm gravity filtered prior to analysis. The chl *a* concentration was 0.08 and 7.0 μg L^{-1} in the Sargasso Sea and Ross Sea, respectively. Absorption spectra in the Sargasso Sea were determined with a Hewlett Packard (HP) 8453 UV-Vis photodiode array spectrophotometer equipped with a 5-cm path length rectangular microliter quartz flow cell; the Sargasso spectrum was referenced against Milli-Q water (for details, see Helms et al., 2008). The small discontinuity at 365 nm is an artifact associated with the HP spectrophotometer (Blough et al., 1993).

Downwelling Attenuation Coefficients

The optical clarity of the water column was reduced considerably from before the onset of the *Phaeocystis antarctica* bloom at station R10 to the end of the cruise at station R14. Before the onset of the *Phaeocystis antarctica* bloom (stations R10 and R13A–R13D), the photic zone exhibited a high degree of optical clarity, characteristic of type 1 open oceanic water (Mobley, 1994), with $K_d(\lambda)$ decreasing exponentially in the UV with increasing wavelength and dominated by absorption by CDOM (Figure 5). Prebloom $K_d(\lambda)$ shown in Figure 5 for station R10 were nearly the same as observed at stations R13A–R13D (data not shown). For station R10, $K_d(\lambda)$ ranged from 0.30 to 0.38 m^{-1} at 305 nm, 0.18– 0.31 m^{-1} at 320 nm, and 0.05–0.15 m^{-1} at 395 nm. Because of low biomass (chl *a* $\leq$ 0.6 $\mu g\ L^{-1}$), the lowest values of $K_d(\lambda)$, and therefore highest degree of optical clarity, were observed in the visible between approximately 450 and 500 nm with $K_d(\lambda)$ ranging from 0.05 to 0.11 m^{-1}. When the bloom started to develop, the optical characteristics of the water, including the spectral structure of $K_d(\lambda)$, changed dramatically. Over an approximately three-week period, values of $K_d(\lambda)$ increased by a factor of six or more at some wavelengths, with peaks observed at two optical channels, 340 ± 10 and 443 ± 10 nm. At stations R13E and R14 (stations A through F) the bloom progressed to the point that the water column was more transparent to some wavelengths in the UV (e.g., 380 nm) relative to wavelengths in the blue portion of the solar spectrum (Figure 5).

Ross Sea Temporal Trends in CDOM

Although UV and visible downwelling attenuation coefficients increased substantially when the *Phaeocystis antarctica* bloom was well developed in the Ross Sea (Figure 5), CDOM absorption coefficient spectra changed very little. To illustrate this point, an absorption coefficient spectrum of a 10-m sample taken before the onset of the bloom at station R10 was compared to a spectrum determined for a 10-m sample at station R14 when the water was visibly green (Figure 6). As can be seen from comparison of these two spectra, as well as from many other spectra not shown here, there was essentially no change in

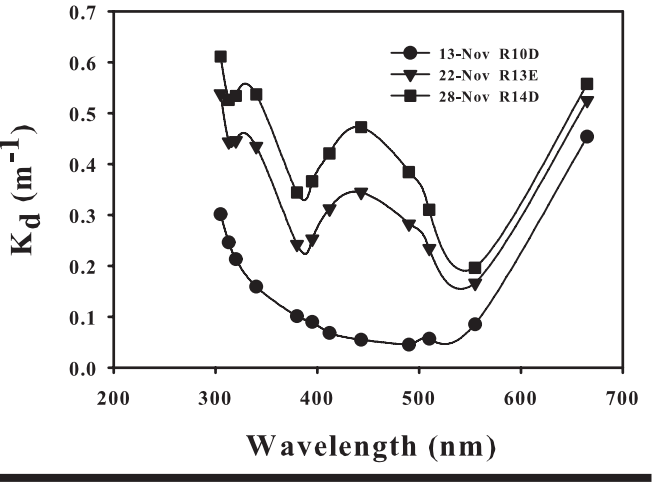

FIGURE 5. Spectral downwelling attenuation coefficients derived from PUV-2500 and PRR-600 profiles both before the *Phaeocystis antarctica* bloom (station R10D, circles) and during the development of the bloom (station R13E, triangles; station R14D, squares). Lines connecting the data do not represent a mathematical fit of the data. Water column profile cast locations are as follows: R10D, 13 November 2005 New Zealand (NZ) time at 76°5.74′S, 170°15.70′W; R13E, 22 November 2005 NZ time at 77°5.20′S, 177°24.49′W; and R14D, 28 November 2005 NZ time at 77°3.61′S, 178°49.06′E. All optical profiles were conducted at approximately 1200 local noon NZ time.

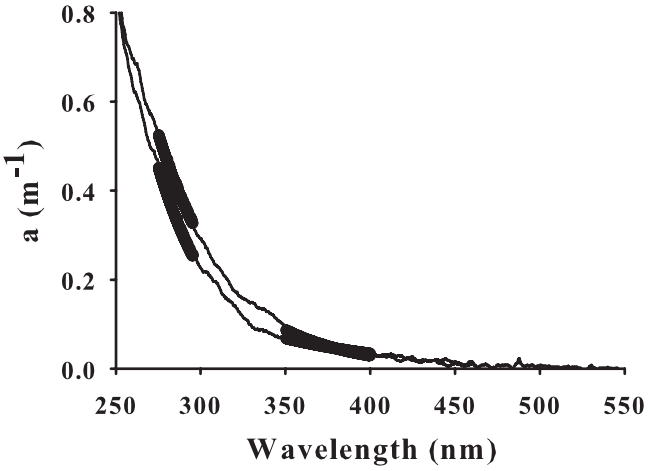

FIGURE 6. Spectral absorption coefficients plotted for 10-m samples from stations R10A (lower spectrum) and R14F (upper spectrum); latitude-longitude data for these stations are given in the Figure 8 caption. Thick lines represent the best fit of the data from 275 to 295 nm and 350 to 400 nm, employing nonlinear regression analysis (equation 2). For station R10A, $S_{275–295}$ = 0.0280 ± 0.0003 nm^{-1} (r^2 = 0.997) and $S_{350–400}$ = 0.0115 ± 0.0003 nm^{-1} (r^2 = 0.904). For station R14F, $S_{275–295}$ = 0.0237 ± 0.0004 nm^{-1} (r^2 = 0.986) and $S_{350–400}$ = 0.0117 ± 0.0005 nm^{-1} (r^2 = 0.916).

absorption coefficients or spectral slopes ($S_{350–400}$) at wavelengths greater than approximately 350 nm. At shorter wavelengths, absorption coefficients and spectral slopes ($S_{275–295}$) varied by 15%–30%, but with no consistent pattern among the many samples analyzed during a period when K_d(340 and 443) and chl *a* changed by more than a factor of 6 and 100, respectively.

Although there were generally only small changes in a_λ spectra and *S*, there was an indication of a discernable increase in absorption coefficients in the vicinity of 330–350 nm seen in a few sample spectra (station R14), with the presence of a small peak (or shoulder) noted in some cases. Previous results in the literature suggest that this peak may be due to the presence of MAA in the dissolved phase, possibly stemming from release by *Phaeocystis antarctica,* either through grazing, viral lysis, or direct release. The MAA are one of the primary UV-absorbing compounds detected in *Phaeocystis antarctica* (e.g., Riegger and Robinson, 1997; Moisan and Mitchell, 2001), and it would not be unreasonable for there to be some algal release of MAA into the dissolved phase. However, it is also possible that this UV absorption peak was an artifact of sample filtration (cf. Laurion et al., 2003). While artifacts associated with sample filtration were not rigorously tested in this study, they are probably minimal because we prescreened water by gravity through 20-μm Nitex mesh to remove large aggregates and *Phaeocystis* colonies and then used gravity (hydrostatic) pressure for filtration through a 0.2-μm AS 75 POLYCAP filter. When gentle vacuum filtration was tested on samples collected during the bloom, we often observed a 330- to 350-nm peak that was not seen in CDOM spectra of the same samples that were prescreened and gravity filtered. Vacuum filtration is not recommended and may explain the presence of a peak in spectra for some samples that were analyzed during a bloom in Marguerite Bay along the Antarctic Peninsula (Patterson, 2000).

The striking lack of change in CDOM spectra and spectral slopes during the development of the *Phaeocystis antarctica* bloom was also seen in temporal trends in surface a_λ. Using 340 nm as an example, surface values of a_{340} in the upper 10 m did not appreciably change from 8 November (0.0782 m^{-1}) to 29 November (0.0837 m^{-1}), while over the same time frame, chl *a* changed by more than a factor of 100 from 0.084 to 8.45 μg L^{-1} (Figure 7A). As with 340 nm, no significant changes in a_λ were observed at other wavelengths during the development of the bloom. Even though CDOM absorption coefficients did not change over time, downwelling attenuation coefficients increased dramatically (Figure 7B),

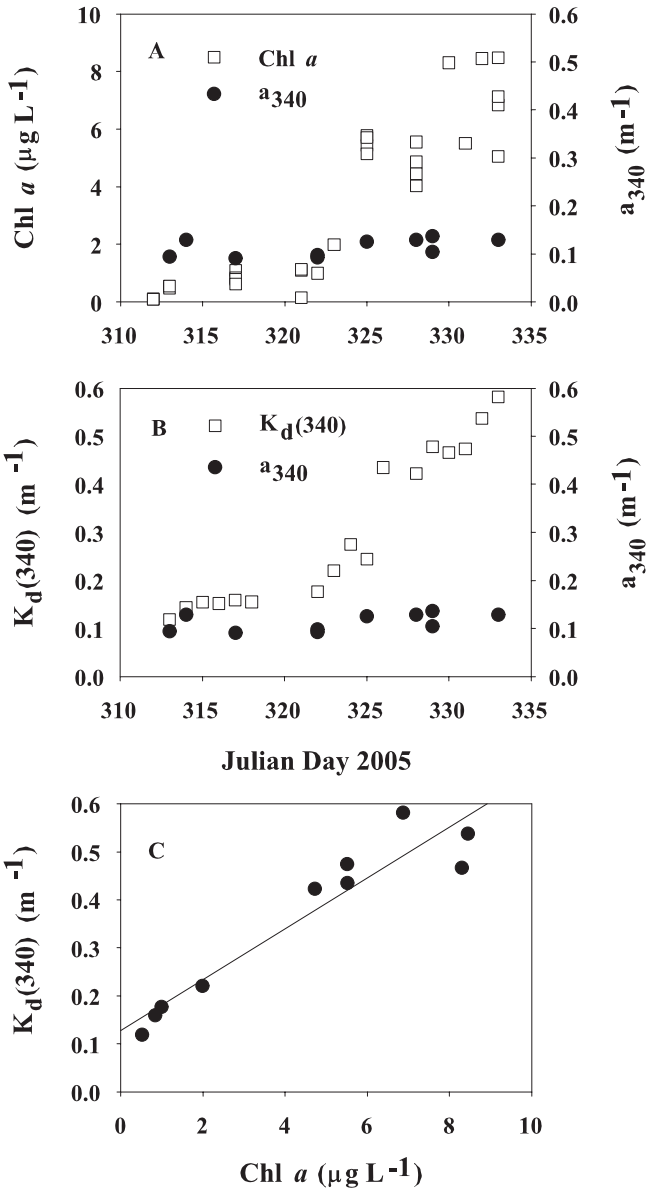

FIGURE 7. Temporal trends in (A) surface chl *a* and a_{340} and (B) K_d(340) and a_{340} from 8 November to 29 November 2005 (NZ time) in the Ross Sea, Antarctica. (C) Chlorophyll *a* plotted against K_d(340). In Figure 7C, the line denotes the best fit obtained from linear correlation analysis: $r^2 = 0.900$, $K_d(340) = 0.053\text{chl } a + 0.128$

paralleling increases in chl *a* (Figure 7C), especially in the vicinity of 340 and 443 nm (Figure 5), corresponding to particulate MAA and chl *a* absorption, respectively. The strong correlation between K_d(340) and chl *a* shown in Figure 7C was also seen when K_d(443) was plotted against chl *a* ($r^2 = 0.937$, data not shown). The nonzero

y-intercept in Figure 7C denotes the background $K_d(340)$ signal at very low chl *a* due to water, CDOM, and particles in the Ross Sea.

The lack of a clear temporal trend noted in a_λ surface values during the *Phaeocystis antarctica* bloom in November 2005 was also evident in a_λ and spectral slope depth profiles (Figures 8 and 9, respectively). Although we obtained multiple profiles at each station, results for only four CTD casts are shown in Figures 8 and 9 for clarity, with at least one CTD profile depicted for each main hydrostation (R10, R13, and R14). The absorption coefficient at 300 nm varied from approximately 0.18 to 0.30 m^{-1} in the upper 100 m, with no temporal trend observed; some of the lowest and highest values were observed early and late in the cruise (Figure 8A). In the upper 50 m, later in the cruise, a_{340} showed somewhat higher values at stations R13E and R14F compared to stations R10 and R13A (Figure 8B), as did chl *a* (Figure 8C). However, while a_{340} increased by 40%–60%, chl *a* increased by more than two orders of magnitude. It was therefore not surprising that variations in a_{340} did not correlate well with changes in chl *a* ($r^2 = 0.384$), as shown in Figure 8D.

Spectral slopes also did not vary with any consistent trend. $S_{275\text{-}295}$ showed less than 25% variation over depth and time, ranging from ~0.023 to 0.031 nm^{-1} (average 0.027 nm^{-1}, $n = 58$, 7% RSD) during the cruise. Trends in $S_{350–400}$ were more variable (range 0.009–0.017 nm^{-1}, average 0.012 nm^{-1}, $n = 58$, 15% RSD) but still showed no consistent trend with depth or time (Figure 9A and 9B). This variability was also seen in the ratio of the spectral slopes (Figure 9C), which showed no correlation to chl *a* ($r^2 = 0.143$; Figure 9D).

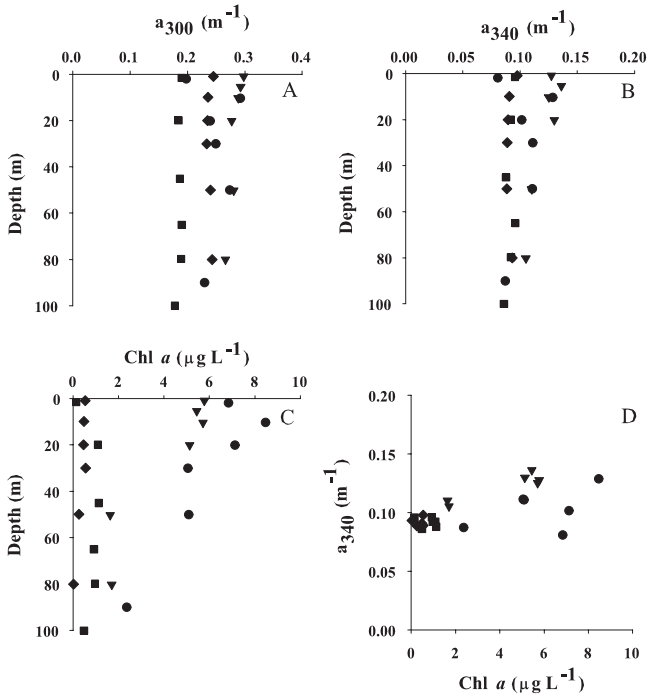

FIGURE 8. Depth profiles of (A) absorption coefficient at 300 nm, (B) absorption coefficient at 340 nm, and (C) chl *a*. (D) Plot of a_{340} versus chl *a*; linear correlation result is $a_{340} = 0.0046\text{chl } a + 0.091$ with $r^2 = 0.384$. Symbols are: diamonds, station R10A (CTD cast at 0754 local NZ time on 10 November 2005; 76°13.85′S, 170°18.12′W); squares, station R13A (CTD cast at 0817 local NZ time on 18 November 2005; 77°35.16′S, 178°34.57′W); triangles, station R13E (CTD cast at 0823 local NZ time on 22 November 2005; 77°12.61′S, 177°23.73′W); and circles, station R14F (CTD cast at 0734 local NZ time on 30 November 2005; 77°15.35′S, 179°15.35′E).

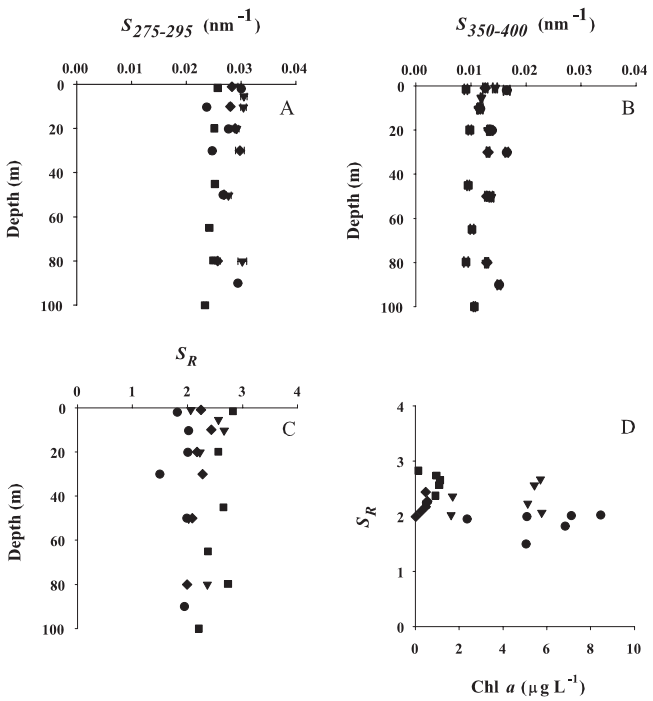

FIGURE 9. Depth profiles of (A) CDOM spectral slope from 275 to 295 nm, (B) CDOM spectral slope from 350 to 400 nm, and (C) the spectral slope ratio ($S_{275–295}$:$S_{350–400}$). Horizontal error bars denote the standard deviation. (D) Spectral slope ratio (S_R) plotted against chl *a*; linear correlation results were $S_R = -0.0447\text{chl } a + 2.37$, with $r^2 = 0.143$ (line not shown). For all four panels, symbols are: diamonds (station R10A), squares (station R13A), triangles (station R13E), and circles (station R14F). Cast times and station locations are given in Figure 8 caption.

DISCUSSION

CDOM absorption coefficients in the Southern Ocean and Ross Sea were consistently low throughout the cruise and along the transect south from New Zealand, with values significantly less than unity at wavelengths ≥300 nm (e.g., 0.15–0.32 m^{-1} at 300 nm). The a_λ values determined in this study are slightly lower than values reported in the Weddell–Scotia Sea confluence (Yocis et al., 2000) and along the Antarctic Peninsula (Sarpal et al., 1995; Yocis et al., 2000) (a_{300}, range 0.19–0.58 m^{-1}) and are similar to values obtained on a 2004–2005 Ross Sea cruise (a_{300}, range ~0.29–0.32 m^{-1}) during the latter stages of the *Phaeocystis antarctica* bloom and transition to a diatom-dominated bloom (Kieber et al., 2007). These published findings, along with results from our transect study and Ross Sea sampling, suggest that relatively low values of a_λ are a general feature of Antarctic waters. By comparison, a_{300} values in the Bering Strait–Chukchi Sea are higher, ranging from 0.3 to 2.1 m^{-1}, with an average of 1.1 m^{-1} ($n = 62$) (Ferenac, 2006). Similarly high a_{300} values in the Greenland Sea (Stedmon and Markager, 2001) suggest that a_λ values in the Antarctic are generally lower than those in Arctic waters, perhaps due to terrestrial inputs of DOM in the Arctic (Opsahl et al., 1999) that are lacking in the Antarctic.

Although Ross Sea absorption coefficients were similar to those in the Sargasso Sea at longer wavelengths >350 nm, absorption coefficient spectra were different in the Ross Sea at shorter wavelengths (Figure 4), with higher a_λ seen between approximately 290 and 350 nm. To illustrate this point further, we computed a_{325} on all casts and depths (in the upper 140 m) during our cruise ($n = 68$) in order to directly compare them to results obtained by Nelson et al. (2007) in the Sargasso Sea. The a_{325} values obtained during the *Phaeocystis antarctica* bloom were, on average (± SD) 0.142 (±0.017) and 0.153 (±0.023) m^{-1} (with an RSD of 12% and 15%) before and during the bloom, respectively, with no temporal trends noted. If we consider a_{325} before the bloom (0.142 m^{-1}) and subtract the calculated contribution due to nitrate (present at 30 μM in the photic zone), then the average a_{325} value due to CDOM is 0.120 m^{-1}. This is approximately a factor of 2.5 higher than a_{325} values reported by Nelson et al. (2007) in the surface Sargasso Sea (~0.05 m^{-1} at 325 nm) and reported by Morel et al. (2007) in the South Pacific gyre.

While our a_{325} values are higher than those Nelson et al. (2007) found in the Sargasso Sea, they are comparable to those Nelson et al. (2007) reported in the Subpolar Gyre (~0.14–0.26 m^{-1}), consistent with a slight poleward trend of increasing a_{325} in open ocean waters due to a poleward decrease in CDOM photolysis rates and an increase in mixed layer depth (Nelson and Siegel, 2002). However, since not all wavelengths showed the same difference between samples (see Figure 4; e.g., a_λ <290 nm were smaller in the Ross Sea compared to the Sargasso Sea), care should be taken in extrapolating trends for all wavelengths given that there are likely regional differences in spectral shapes due to differences in CDOM source and removal pathways.

The supposition that CDOM photobleaching rates are slow in Antarctic waters is supported by field evidence. When 0.2-μm-filtered Ross Sea seawater samples in quartz tubes were exposed to sunlight for approximately eight hours, no measurable CDOM photobleaching was observed. This contrasts results from the Sargasso Sea or other tropical and temperate waters, where ~10% loss in CDOM absorption coefficients is observed after six to eight hours of exposure to sunlight (D. J. Kieber, unpublished results). This difference is likely driven by lower actinic fluxes at polar latitudes. However, differences in DOM reactivity cannot be ruled out. In addition to direct photobleaching experiments, no evidence for photobleaching was observed in a_{CDOM} depth profiles. At 300 nm, for example, absorption coefficients were uniform in the upper 100 m or showed a slight increase near the surface (Figure 8), a trend that is opposite of what would be expected if CDOM photolysis (bleaching) controlled near-surface a_λ. It is also possible that mixing masked photobleaching, but this was not evaluated.

Absorption Coefficient at 443 nm

Understanding what controls spatial and temporal trends in near-surface light attenuation is critical to accurately interpret remotely sensed ocean color data from the Sea-viewing Wide Field-of-view Sensor (SeaWiFS) or future missions (see Smith and Comiso, 2009, this volume). One of the primary limitations in using satellite ocean color data to model CDOM distributions is the lack of directly measured CDOM spectra in the oceans for model calibration and validation, particularly in open oceanic environments and polar waters (Siegel et al., 2002). The 443 waveband corresponds to the chl *a* absorption peak and is often used in bio-optical algorithms for pigment concentrations, although model estimates suggest that CDOM and detrital absorption account globally for >50% of total nonwater absorption at this wavelength (Siegel et al., 2002). During

our cruise, chl *a* concentrations varied one-hundred-fold, while a_{443} varied approximately 35% and showed no correlation to chl *a*. In the upper water column, a_{443} was, on average (± SD) 0.032 (±0.011) m^{-1}, with no difference observed in prebloom values (0.031 ± 0.011 m^{-1}) compared to values obtained during the bloom (0.033 ± 0.012 m^{-1}). These observations fall within the range of wintertime zonally predicted values for southern latitudes between approximately 60° and 75°S (~0.009–0.05 m^{-1}) (Siegel et al., 2002) and suggest that the phytoplankton bloom is not directly responsible for the observed CDOM absorption.

While we do not have direct observations to calculate the contribution of CDOM absorption to total absorption, $K_d(\lambda)$ values allow us to assess the contribution of CDOM to total light attenuation. $K_d(\lambda)$ calculated from upper ocean optical profiles is the sum of component $K_d(\lambda)$ from pure water, CDOM, and particulate material (phytoplankton and detritus). The contribution from particulate material can be determined using $K_d(\lambda)$ from pure water (Morel and Maritorena, 2001) in conjunction with measured CDOM absorption coefficients. To a first approximation the majority of the particulate matter is expected to be living phytoplankton, as the Ross Sea is spatially removed from sources of terrigenous material. At the prebloom station R10A, the chl *a* concentration in the upper 30 m was, on average (±SD), 0.51 (±0.04) μg L^{-1} and $K_d(443)$ was relatively low (0.0684 m^{-1}). Pure water contributed 14.5% of the total attenuation at 443 nm while CDOM accounted for 42.8% (±4.7%) (avg ± RSD) of the nonwater absorption, with 57.2% (±4.7%) accounted for by particles. At the bloom station R14D, the average chl *a* concentration was an order of magnitude greater (6.87 ± 1.4 μg L^{-1}), and pure water contributed 2.1% of the total attenuation at 443 nm. Chromophoric dissolved organic matter accounted for only 3.5% (±0.9%) of the total nonwater attenuation, with particles contributing the remaining 96.5% (±0.9%). Not surprisingly, this confirms that the attenuation of blue and green wavelengths was dominated by particles and not by dissolved constituents during the bloom.

Many of the current suite of satellite algorithms (e.g., OC4v4, O'Reilly et al., 2000) have been shown to poorly predict chl *a* in the Southern Ocean, potentially because of the unique optical properties of large *Phaeocystis antarctica* colonies or the assumption that water column optical properties covary with chl *a* (e.g., Siegel et al., 2005). Our results confirm that semianalytical approaches, which individually solve for optical components, are necessary to describe the decoupling of CDOM and particulate material during *Phaeocystis antarctica* blooms in the Ross Sea and ultimately allow accurate chl *a* retrievals.

Spectral Slope

The spectral slope (*S*) varies substantially in natural waters, and it has been used to provide information about the source, structure, and history of CDOM (Blough and Del Vecchio, 2002). However, while spectral slopes have been reported in the literature for a range of natural waters, they are nearly impossible to compare because of differences in how *S* values have been determined and because different wavelength ranges have been considered (Twardowski et al., 2004). Indeed, when we employed a nonlinear fitting routine to determine the spectral slope over several broad wavelength ranges, a range of *S* values was obtained for the same water sample [e.g., 0.0159 nm^{-1} (290–500 nm), 0.0124 nm^{-1} (320–500 nm), 0.0118 nm^{-1} (340–500 nm), 0.0133 nm^{-1} (360–500 nm), 0.0159 nm^{-1} (380–500 nm), 0.0164 nm^{-1} (400–500 nm)]. These variations in the slope indicate that Antaractic a_λ spectra do not fit a simple exponential function, as also observed by Sarpal et al. (1995) for samples along the Antarctic Peninsula. Therefore, instead of computing *S* over relatively broad wavelength ranges, we chose instead to compute *S* over two relatively narrow wavelength ranges proposed by Helms et al. (2008), 275–295 nm and 350–400 nm. These wavelength ranges were chosen because they can be determined with high precision and they are less prone to errors in how the data are mathematically fit relative to broad wavelength ranges (e.g., 290–700 nm; Helms et al., 2008). Additionally, the ratio, S_R, for these two wavelength ranges should facilitate comparison of different natural waters. In our study, the spectral slope between 275 and 295 nm was in all cases significantly higher than at 350–400 nm (~0.028 nm^{-1} versus ~0.013 nm^{-1}, respectively), and S_R was low, ranging between 1 and 3, with an average value of 2.32 (e.g., Figure 9C).

Our S_R are similar to coastal values observed in the Georgia Bight (avg ± SD: 1.75 ± 0.15) and elsewhere even though a_λ in coastal areas are much higher than we observed in the Ross Sea (e.g., >1 m^{-1} versus <0.3 m^{-1} at 300 nm, respectively). Likewise, the S_R values we found in the Ross Sea are much lower than those observed in open oceanic sites, where values as high as 9 or more have been observed (Helms et al., 2008). Helms et al. (2008) found a strong positive correlation between S_R and the relative proportion of low molecular weight DOM versus high molecular weight (HMW) DOM in the sample. If the results of Helms et al. can be extrapolated to Antarctic waters, then

our low S_R results would suggest that the Ross Sea samples contained a relatively high proportion of HMW DOM compared to what is observed in oligotrophic waters. The relatively higher molecular weight DOM and low S_R in the Ross Sea may be related to the lower photobleaching rates that are observed in the Antarctic, since photobleaching is the main mechanism to increase S_R and remove HMW DOM (Helms et al., 2008).

CDOM Source

The CDOM present in coastal areas near rivers and in estuaries in subtropical-temperate and northern boreal latitudes is predominantly of terrestrial origin (e.g., Blough et al., 1993; Blough and Del Vecchio, 2002; Rochelle-Newall and Fisher, 2002a), but in the open ocean, as in the Antarctic, terrigenous CDOM is only a minor component of the total DOM pool (Opsahl and Benner, 1997; Nelson and Siegel, 2002).

Phytoplankton are expected to be the main source of CDOM in the open ocean, although they are not thought to be directly responsible for CDOM production (Bricaud et al., 1981; Carder et al., 1989; Del Castillo et al., 2000; Nelson et al., 1998, 2004; Rochelle-Newall and Fisher 2002b; Ferenac, 2006). Our results are consistent with this finding (Figure 7). With no substantial grazing pressure (Rose and Caron, 2007, and as noted by our colleagues D. Caron and R. Gast during our cruise to the Ross Sea in early November 2005) and very low bacterial activity (Ducklow et al., 2001; Del Valle et al., in press), it is not surprising that CDOM a_{300} and a_{340} changed very little during the bloom. In fact, a_{300} did not apparently increase even during the latter stages of the Ross Sea *Phaeocystis antarctica* bloom when the microbial activity was higher (Kieber et al., 2007: fig. 5). This finding is rather remarkable since DOC is known to increase by ~50% during the *Phaeocystis antarctica* bloom from ~42 to >60 μM in the Ross Sea (Carlson et al., 1998). We also observed a DOC increase during our cruise from background levels (~43 μM at 130 m) to 53-μM DOC near the surface (based on one DOC profile obtained at our last station, R14F, on 30 November 2005). This difference suggests that the DOC increase was due to the release of nonchromophoric material by *Phaeocystis antarctica*. Field results support this supposition, showing that the main DOC produced by *Phaeocystis antarctica* is carbohydrates (Mathot et al., 2000).

The temporal and spatial decoupling between DOC and CDOM cycles in the Ross Sea photic zone indicate that CDOM was produced later in the season or elsewhere in the water column. Since evidence from Kieber et al. (2007) suggests that additional CDOM did not accumulate later in the season, it was likely produced elsewhere. Previous studies have shown that sea ice is a rich source of CDOM (Scully and Miller, 2000; Xie and Gosselin, 2005). It is therefore possible that the pack ice along the edges of the Polynya was an important source of CDOM in the photic zone, especially the bottom of the ice, which was visibly light brown with ice algae. It is also possible that CDOM was produced below the photic zone and reached the photic layer via vertical mixing. Several lines of evidence indicate that Ross Sea *Phaeocystis antarctica* may be exported out of the photic zone (DiTullio et al., 2000; Rellinger et al., in press) and perhaps reach the ocean floor (~900 m) (DiTullio et al., 2000), as seen in the Arctic. Arctic algal blooms often occur in the early spring when the water is still too cold for significant zooplankton grazing and bacterial growth (Overland and Stabeno, 2004). As a consequence, the algae sink out of the photic zone and settle to the ocean floor rather than being consumed, thereby providing a DOM source for long-term CDOM production in dark bottom waters. A similar phenomenon may occur in the Ross Sea. The possibility that CDOM may be generated in deep waters, with no photobleaching, might explain the high photosensitizing capacity of this CDOM for important reactions like DMS photolysis (Toole et al., 2004).

Deepwater production of CDOM in the Ross Sea would explain why our a_{325} values are comparable to those observed by Nelson et al. (2007: figs. 8–9) in deep water (~0.1–0.2 m^{-1}) and nearly the same as would be predicted on the basis of values in Antarctic Bottom Water and Antarctic Intermediate Water (average of ~0.13–0.14 m^{-1}). Although speculative, it is possible that CDOM is exported from the Southern Ocean to deep waters at temperate-subtropical latitudes, which would be consistent with CDOM as a tracer of oceanic circulation (Nelson et al., 2007).

CONCLUSIONS

Despite the necessity of understanding the spatial and temporal distributions of CDOM for remote sensing, photochemical, and biogeochemical applications, few measurements have been made in the Southern Ocean. Our results indicate that Antarctic CDOM shows spectral properties that are intermediate between what is observed

in coastal environments and properties observed in the main oceanic gyres. We suggest this trend is largely due to slow photobleaching rates and shading from *Phaeocystis antarctica* and other bloom-forming species that contain substantial MAA.

While CDOM spectral absorption coefficients are low in Antarctic waters, they are generally higher than surface water a_λ in low-latitude, open-ocean waters, such as the Sargasso Sea, supporting the supposition of a poleward increase in a_{CDOM} in the open ocean. Our results suggest that CDOM in the Ross Sea is not coupled directly to algal production of organic matter in the photic zone. This indicates that case I bio-optical algorithms, in which all in-water constituents and the underwater light field are modeled to covary with chl *a* (e.g., Morel and Maritorena, 2001), are inappropriate. The decoupling of the phytoplankton bloom and CDOM dynamics indicates that CDOM is produced from sea ice or the microbial degradation of algal-derived dissolved organic matter that was exported out of the photic zone. Ross Sea CDOM absorption coefficients are similar in magnitude to values in Antarctic-influenced deep waters of the North Atlantic (Nelson et al., 2007), suggesting long-range transport of CDOM produced in the Ross Sea via Antarctic Intermediate and Bottom Water.

Acknowledgments

This work was supported by the NSF (grant OPP-0230499, DJK; grant OPP-0230497, RPK). Any opinions, findings, and conclusions or recommendations expressed in this paper are those of the authors and do not necessarily reflect the views of the NSF. The authors gratefully acknowledge the chief scientists for the October–December 2005 Ross Sea cruise, Wade Jeffery (University of West Florida) and Patrick Neale (Smithsonian Environmental Research Center). Thanks are also extended to Patrick Neale, Wade Jeffery, and their research groups for collection of the optics profiles, and the captain and crew of the *Nathanial B. Palmer* for technical assistance. We also thank Joaquim Goes (Bigelow Laboratory for Ocean Sciences), Helga do S. Gomes (Bigelow Laboratory for Ocean Sciences), Cristina Sobrino (Smithsonian Environmental Research Center), George Westby (State University of New York, College of Environmental Science and Forestry: SUNY-ESF), John Bisgrove (SUNY-ESF), Hyakubun Harada (Dauphin Island Sea Lab, University of South Alabama), Jennifer Meeks (Dauphin Island Sea Lab, University of South Alabama), Jordan Brinkley (SUNY-ESF), and Daniela del Valle (Dauphin Island Sea Lab, University of South Alabama) for their technical help with sampling during this study.

LITERATURE CITED

Becquevort, S., and W. O. Smith Jr. 2001. Aggregation, Sedimentation and Biodegradability of Phytoplankton-Derived Material During Spring in the Ross Sea, Antarctica. *Deep-Sea Research, Part II*, 48: 4155–4178.

Blough, N. V., and R. Del Vecchio. 2002. "Chromophoric DOM in the Coastal Environment." In *Biogeochemistry of Marine Dissolved Organic Matter*, ed. D. A. Hansell and C. A. Carlson, pp. 509–546. San Diego: Academic Press.

Blough, N. V., O. C. Zafiriou, and J. Bonilla. 1993. Optical Absorption Spectra of Waters from the Orinoco River Outflow: Terrestrial Input of Colored Organic Matter to the Caribbean. *Journal of Geophysical Research*, 98:2271–2278.

Bricaud, A., A. Morel, and L. Prieur. 1981. Absorption by Dissolved Organic Matter of the Sea (Yellow Substance) in the UV and Visible Domains. *Limnology and Oceanography*, 26:43–53.

Carder, K. L., R. G. Steward, G. R. Harvey, and P. B. Ortner. 1989. Marine Humic and Fulvic Acids: Their Effects on Remote Sensing of Ocean Chlorophyll. *Limnology and Oceanography*, 34:68–81.

Carlson, C. A., H. W. Ducklow, D. A. Hansell, and W. O. Smith Jr. 1998. Organic Carbon Partitioning during Spring Phytoplankton Blooms in the Ross Sea Polynya and the Sargasso Sea. *Limnology and Oceanography*, 43:375–386.

Carlson, C. A., D. A. Hansell, E. T. Peltzer, and W. O. Smith Jr. 2000. Stocks and Dynamics of Dissolved and Particulate Organic Matter in the Southern Ross Sea, Antarctica. *Deep-Sea Research*, *Part II* 47:3201–3225.

Caron, D. A., M. R. Dennett, D. J. Lonsdale, D. M. Moran, and L. Shalapyonok. 2000. Microzooplankton Herbivory in the Ross Sea, Antarctica. *Deep-Sea Research*, *Part II*, 47:3249–3272.

Chen, R. F., P. Bissett, P. Coble, R. Conmy, G. B. Gardner, M. A. Moran, X. Wang, M. W. Wells, P. Whelan, and R. G. Zepp. 2004. Chromophoric Dissolved Organic Matter (CDOM) Source Characterization in the Louisiana Bight. *Marine Chemistry*, 89:257–272.

Del Castillo, C. E., F. Gilbes, P. G. Coble, and F. E. Muller-Karger. 2000. On the Dispersal of Riverine Colored Dissolved Organic Matter over the West Florida Shelf. *Limnology and Oceanography*, 45:1425–1432.

del Valle, D. A., D. J. Kieber, D. A. Toole, J. C. Brinkley, and R. P. Kiene. In press. Biological Consumption of Dimethylsulfide (DMS) and Its Importance in DMS Dynamics in the Ross Sea, Antarctica. *Limnology and Oceanography*.

Del Vecchio, R., and N. V. Blough. 2002. Photobleaching of Chromophoric Dissolved Organic Matter in Natural Waters: Kinetics and Modeling. *Marine Chemistry*, 78:231–253.

———. 2004. Spatial and Seasonal Distribution of Chromophoric Dissolved Organic Matter and Dissolved Organic Carbon in the Middle Atlantic Bight. *Marine Chemistry*, 89:169–187.

DiTullio, G. R., J. M. Grebmeier, K. R. Arrigo, M. P. Lizotte, D. H. Robinson, A. Leventer, J. P. Barry, M. L. VanWoert, and R. B. Dunbar. 2000. Rapid and Early Export of *Phaeocystis antarctica* Blooms in the Ross Sea, Antarctica. *Nature*, 404:595–598.

Ducklow, H., C. Carlson, M. Church, D. Kirchman, D. Smith, and G. Steward. 2001. The Seasonal Development of the Bacterioplankton Bloom in the Ross Sea, Antarctica, 1994–1997. *Deep-Sea Research*, *Part II*, 48:4199–4221.

Ferenac, M. A. 2006. Optical Properties of Chromophoric Dissolved Organic Matter (CDOM) in the Bering Strait and Chukchi Sea. Master's thesis, College of Environmental Science and Forestry, State University of New York, Syracuse.

Hebling, E. W., and H. Zagarese, eds. 2003. *UV Effects in Aquatic Organisms and Ecosystems*. Comprehensive Series in Photochemical and Photobiological Sciences, Vol. 1. Cambridge, U.K.: Royal Society of Chemistry.

Helms, J. R., A. Stubbins, J. D. Ritchie, E. C. Minor, D. J. Kieber, and K. Mopper. 2008. Absorption Spectral Slopes and Slope Ratios as Indicators of Molecular Weight, Source and Photobleaching of Chromophoric Dissolved Organic Matter. *Limnology and Oceanography*, 53:955–969.

Kieber, D. J., B. M. Peake, and N. M. Scully. 2003. "Reactive Oxygen Species in Aquatic Ecosystems." In *UV Effects in Aquatic Organisms and Ecosystems*, ed. E.W. Hebling and H. Zagarese, pp. 251–288. Comprehensive Series in Photochemical and Photobiological Sciences, Vol. 1. Cambridge, U.K.: Royal Society of Chemistry.

Kieber, D. J., D. A. Toole, J. J. Jankowski, R. P. Kiene, G. R. Westby, D. A. del Valle, and D. Slezak. 2007. Chemical "Light Meters" for Photochemical and Photobiological Studies. *Aquatic Sciences*, 69: 360–376.

Kiene, R. P., D. J. Kieber, D. Slezak, D. A. Toole, D. A. Del Valle, J. Bisgrove, J. Brinkley, and A. Rellinger. 2007. Distribution and Cycling of Dimethylsulfide, Dimethylsulfoniopropionate, and Dimethylsulfoxide During Spring and Early Summer in the Southern Ocean South of New Zealand. *Aquatic Sciences,* 69:305–319.

Laurion, I., F. Blouin and S. Roy. 2003. The Quantitative Filter Technique for Measuring Phytoplankton Absorption: Interference by MAAs in the UV Waveband. *Limnology and Oceanography: Methods*, 1:1–9.

Mathot, S., W. O. Smith Jr., C. A. Carlson, D. L. Garrison, M. M. Gowing, and C. L. Vickers. 2000. Carbon Partitioning Within *Phaeocystis antarctica* (Prymnesiophyceae) Colonies in the Ross Sea, Antarctica. *Journal of Phycology*, 36:1049– 1056.

Mobley, C. D. 1994. *Light and Water: Radiative Transfer in Natural Waters*. San Diego: Academic Press.

Moisan, T. A., and B. G. Mitchell. 2001. UV Absorption by Mycosporine-Like Amino Acids in *Phaeocystis antarctica* Karsten Induced by Photosynthetically Available Radiation. *Marine Biology*, 138: 217–227.

Morel, A., and S. Maritorena. 2001. Bio-optical Properties of Oceanic Waters: A Reappraisal. *Journal of Geophysical Research*, 106: 7163–7180.

Morel, A., B. Gentili, H. Claustre, M. Babin, A. Bricaud, J. Ras, and F. Tieche. 2007. Optical Properties of the "Clearest" Natural Waters. *Limnology and Oceanography*, 52:217–229.

Nelson, N. B., and D. A. Siegel. 2002. "Chromophoric DOM in the open ocean." In *Biogeochemistry of Marine Dissolved Organic Matter,* ed. D. A. Hansell and C. A. Carlson, pp. 547–578. San Diego: Academic Press.

Nelson, N. B., D. A. Siegel, and A. F. Michaels. 1998. Seasonal Dynamics of Colored Dissolved Material in the Sargasso Sea. *Deep-Sea Research, Part I* 45:931–957.

Nelson, N. B., C. A. Carlson, and D. K. Steinberg. 2004. Production of Chromophoric Dissolved Organic Matter by Sargasso Sea Microbes. *Marine Chemistry*, 89:273–287.

Nelson, N. B., D. A. Siegel, C. A. Carlson, C. Swan, W. M. Smethie Jr., and S. Khatiwala. 2007. Hydrography of Chromophoric Dissolved Organic Matter in the North Atlantic. *Deep-Sea Research*, *Part I* 54:710–731.

Opsahl, S., and R. Benner. 1997. Distribution and Cycling of Terrigenous Dissolved Organic Matter in the Ocean. *Nature*, 386:480–482.

Opsahl, S., R. Benner, and R. M. W. Amon. 1999. Major Flux of Terrigenous Dissolved Organic Matter through the Arctic Ocean. *Limnology and Oceanography*, 44:2017–2023.

O'Reilly, J. E., S. Maritorena, D. A. Siegel, M. C. O'Brien, D. A. Toole, F. P. Chavez, P. Strutton, G. F. Cota, S. B. Hooker, C. R. McClain, K. L. Carder, F. Muller-Karger, L. Harding, A. Magnuson, D. Phinney, G. F. Moore, J. Aiken, K. R. Arrigo, R. Letelier, and M. Culver. 2000. Ocean Color Chlorophyll-*a* Algorithms for SeaWiFS, OC2 and OC4: Version 4. In *SeaWiFS Postlaunch Calibration and Validation Analyses: Part 3*, ed. S. B. Hooker and E. R. Firestone, pp. 9–23. NASA Technical Memorandum, No. 2000-206892, Volume 11. NASA Goddard Space Flight Center, Greenbelt, Md.

Overland, J. E., and P. J. Stabeno. 2004. Is the Climate of the Bering Sea Warming and Affecting the Ecosystem? *Eos, Transactions, American Geophysical Union*, 85:309–310, 312.

Patterson, K. W. 2000. Contribution of Chromophoric Dissolved Organic Matter to Attenuation of Ultraviolet Radiation in Three Contrasting Coastal Areas. Ph.D. diss., University of California, Santa Barbara.

Qian, J., and K. Mopper. 1996. Automated High-Performance, High-Temperature Combustion Total Organic Carbon Analyzer. *Analytical Chemistry*, 68:3090–3097.

Rellinger, A. N., R. P. Kiene, D. Slezak, D. A. del Valle, H. Harada, J. Bisgrove, D. J. Kieber, and J. Brinkley. In press. Occurrence and Turnover of DMSP and DMS in the Deep Waters of the Ross Sea, Antarctica. *Deep Sea Research, Part I.*

Riegger, L., and D. Robinson. 1997. Photoinduction of UV-Absorbing Compounds in Antarctic Diatoms and *Phaeocystis antarctica*. *Marine Ecology Progress Series*, 160:13–25.

Rochelle-Newall, E. J., and T. R. Fisher. 2002a. Chromophoric Dissolved Organic Matter and Dissolved Carbon in Chesapeake Bay. *Marine Chemistry*, 77:23–41.

———. 2002b. Production of Chromophoric Dissolved Organic Matter Fluorescence in Marine and Estuarine Environments: An Investigation into the Role of Phytoplankton. *Marine Chemistry*, 77: 7–21.

Rose, J. M., and D. A. Caron. 2007. Does Low Temperature Constrain the Growth Rates of Heterotrophic Protists? Evidence and Implications for Algal Blooms in Cold Waters. *Limnology and Oceanography*, 52:886–895.

Sarpal, R. S., K. Mopper, and D. J. Kieber. 1995. Absorbance Properties of Dissolved Organic Matter in Antarctic Waters. *Antarctic Journal of the United States*, 30:139–140.

Schindler, D. W., and P. J. Curtis. 1997. The Role of DOC in Protecting Freshwaters Subjected to Climatic Warming and Acidification from UV Exposure. *Biogeochemistry*, 36:1–8.

Scully, N. M., and W. L. Miller. 2000. Spatial and Temporal Dynamics of Colored Dissolved Organic Matter in the North Water Polynya. *Geophysical Research Letters*, 27:1009–1011.

Siegel, D. A., S. Maritorena, N. B. Nelson, D. A. Hansell, and M. Lorenzi-Kayser. 2002. Global Distribution and Dynamics of Colored Dissolved and Detrital Organic Materials. *Journal of Geophysical Research*, 107:3228, doi:10.1029/2001JC000965.

Siegel, D. A., S. Maritorena, N. B. Nelson, and M. J. Behrenfeld. 2005. Independence and Interdependencies of Global Ocean Color Properties: Reassessing the Bio-optical Assumption, *Journal of Geophysical Research*, 110:C07011, doi:10.1029/2004JC002527.

Smith, W. O., Jr., and J. C. Comiso. 2009. "Southern Ocean Primary Productivity: Variability and a View to the Future." In *Smithsonian at the Poles: Contributions to International Polar Year Science*, ed. I. Krupnik, M. A. Lang, and S. E. Miller, pp. 309–318. Washington, D.C.: Smithsonian Institution Scholarly Press.

Smith, W. O., Jr., J. Marra, M. R. Hiscock, and R. T. Barber. 2000. The Seasonal Cycle of Phytoplankton Biomass and Primary Productivity in the Ross Sea, Antarctica. *Deep-Sea Research*, *Part II*, 47:3119–3140.

Stedmon, C. A., and S. Markager. 2001. The Optics of Chromophoric Dissolved Organic Matter (CDOM) in the Greenland Sea: An Algorithm for Differentiation between Marine and Terrestrially

Derived Organic Matter. *Limnology and Oceanography*, 46: 2087–2093.

Strickland, J. D. H., and T. R. Parsons. 1968. A Practical Handbook of Seawater Analysis. *Bulletin of the Fisheries Research Board of Canada*, 167:1–311.

Toole, D. A., D. J. Kieber, R. P. Kiene, D. A. Siegel, and N. B. Nelson. 2003. Photolysis and the Dimethyl Sulfide (DMS) Summer Paradox in the Sargasso Sea. *Limnology and Oceanography*, 48:1088–1100.

Toole, D. A., D. J. Kieber, R. P. Kiene, E. M. White, J. Bisgrove, D. A. del Valle, and D. Slezak. 2004. High Dimethylsulfide Photolysis Rates in Nitrate-Rich Antarctic Waters. *Geophysical Research Letters*, 31:L11307, doi:10.1029/2004GL019863.

Twardowski, M. S., E. Boss, J. M. Sullivan, and P. L. Donaghay. 2004. Modeling the Spectral Shape of Absorption by Chromophoric Dissolved Organic Matter. *Marine Chemistry*, 89:69–88.

Vähätalo, A. V., and R. G. Wetzel. 2004. Photochemical and Microbial Decomposition of Chromophoric Dissolved Organic Matter during Long (Months-Years) Exposures. *Marine Chemistry*, 89:313–326.

Vodacek, A., N. V. Blough, M. D. DeGrandpre, E. T. Peltzer, and R. K. Nelson. 1997. Seasonal Variation of CDOM and DOC in the Middle Atlantic Bight: Terrestrial Inputs and Photooxidation. *Limnology and Oceanography*, 42:674–686.

Waters, K. J., R. C. Smith, and M. R. Lewis. 1990. Avoiding Ship-Induced Light-Field Perturbation in the Determination of Oceanic Optical Properties. *Oceanography,* 3:18–21.

Xie, H., and M. Gosselin. 2005. Photoproduction of Carbon Monoxide in First-Year Sea Ice in Franklin Bay, Southeastern Beaufort Sea. *Geophysical Research Letters,* 32:L12606. doi:10.1029/2005GL022803.

Yocis, B. H., D. J. Kieber, and K. Mopper. 2000. Photochemical Production of Hydrogen Peroxide in Antarctic Waters. *Deep-Sea Research, Part I* 47:1077–1099.